Reduction of Ni^{2+} by hydrazine in solution for the preparation of nickel nano-particles

ZHIYU LI, CHENGHUI HAN
Lab of Mesoscopic Chemistry, Department of Chemistry, Nanjing University, Nanjing 210093, China; Jiangsu Radio and Television University, Nanjing 210013, China

JIANYI SHEN*
Lab of Mesoscopic Chemistry, Department of Chemistry, Nanjing University, Nanjing 210093, China
E-mail: jyshen@nju.edu.cn

Published online: 12 April 2006

The reduction of Ni^{2+} by hydrazine in solution for the preparation of nickel nano-particles has been studied. It was found that the reactions occur in two stages. The first stage is the reduction of Ni^{2+} by N_2H_4 according to $2Ni^{2+} + N_2H_4 + 4OH^- = 2Ni\downarrow + N_2\uparrow + 4H_2O$, while the second stage consists of two side reactions, the decomposition of hydrazine ($N_2H_4 = N_2\uparrow + 2H_2\uparrow$) and the disproportionation of hydrazine ($3N_2H_4 = N_2\uparrow + 4NH_3\uparrow$) catalyzed by the formed nickel nano-particles. The reaction for the formation of nickel is also catalyzed by nickel as an autocatalytic reaction. Accordingly, a small amount of inducing agent, $NaBH_4$ can be added to initiate the reaction that can then proceed continuously at 288 K. Kinetic study reveals that the reaction orders with respect to Ni^{2+}, N_2H_4 and Ni are 1, 0 and 1, respectively. Thus, the increase of the initial concentration of Ni^{2+} and the amount of inducing agent used accelerate the reaction rate and decrease the consumption of N_2H_4 significantly. Pure nickel nano-particles with high surface areas are produced and the surface area can increase from 18 to 79 m^2/g with the increase of concentration of Ni^{2+} used. The fully understanding of the reaction between Ni^{2+} and hydrazine in solution may provide a new optimized technique to prepare the nickel catalysts with high surface areas, in addition to the currently available techniques for the preparation of Raney nickel and supported nickel catalysts.

1. Introduction

Metal nano-particles have important applications as catalytic and magnetic materials. They can also be used for the preparation of porous metallic ensembles and as fillers for polymers. Different techniques have been used to prepare the metal nano-particles, for example, the reduction of metal oxide or salts [1,2], decomposition of metal carbonyls [1] and reduction in solutions by strong reducing agents [3–9]. The reducing agents reported include potassium borohydrides, sodium hypophosphite and hydrazine, corresponding to the formation of metal borides [3–5], metal phosphides [6–8] and pure metals [9]. In recent years, quite a few publications reported the reduction of metal cations, especially Ni^{2+}, by hydrazine in solutions to produce metallic nano-particles [9–15]. Some authors discussed the reaction mechanism for the reduction of nickel cations by hydrazine [9, 13]. However, these studies on reaction mechanism and kinetics are not intensive and conclusive. In fact, the features of the reduction and factors influencing the reactions are not clearly known so far, so that the choice of the ratio of hydrazine to nickel cation, the reaction temperature and time for the production of nickel nano-particles was not based on the deeply understood reaction mechanism and kinetics. It is known that the reduction of Ni^{2+} in solution by BH_4^-, $H_2PO_2^-$ or N_2H_4 releases gases, and the measurement of the gases evolved versus time gives the reaction kinetics and may also indicate the percentage of side reactions. In this way, we have analyzed the reaction mechanisms and kinetics for the reduction of Ni^{2+} by BH_4^- to form Ni–B nano-particles [5] and by $H_2PO_2^-$ to form Ni-P nano-particles [8]. In this work,

*Author to whom all correspondence should be addressed.
0022-2461
DOI: 10.1007/s10853-005-5874-z

we addressed the reduction of Ni^{2+} by hydrazine in solution. We first analyzed the electrochemistry for the reduction to see how many reactions might be involved. Then, we examined the main reaction for the reduction of Ni^{2+} to form nickel nano-particles and accompanied side reactions. Finally, we determined the reaction kinetics by measuring the gases evolved versus time and found out when and in what extent the main reaction and the side reactions occurred under different reaction conditions.

2. Experimental section

The apparatus used for this work is similar to those used for the preparation of Ni–B and Ni–P nano-particles [5, 8]. For the reduction of Ni^{2+} by hydrazine, a jacketed beaker was used, in which water at constant temperatures from 288 to 323 K was cycled in the outer jacket. According to ref. [14], 1 g $NiCl_2{\cdot}6H_2O$ (0.0042 mol) was dissolved in 7.5 ml 95% ethanol and was added into the beaker. 4 g 50%$N_2H_4{\cdot}H_2O$ (0.04 mol) was mixed with 2.5 g NaOH with stirring and the slurry formed was added into the beaker. The mixture was stirred by a magnetic stirrer. The reaction was initiated by adding a small amount of inducing agent, $NaBH_4$, which reduced Ni^{2+} into Ni-B nano-particles that catalyzed the reaction between Ni^{2+} and hydrazine. The gases evolved during the reaction first passed 200 ml de-ionized water in order to absorb ammonia produced and the pH of the ammonia solution was determined versus time so that the production of ammonia can be monitored. The volume of gases that can not be absorbed by water (N_2 and H_2) was measured also versus time. Ammonia, N_2 and H_2 are the only gases produced during the reduction of Ni^{2+} by N_2H_4 and the kinetics of evolving these gases is a measure of the kinetics for the main reaction (reduction of Ni^{2+}) and other side reactions (e.g., decomposition of N_2H_4 catalyzed by Ni surface).

A black precipitate was formed during the reduction of Ni^{2+} by N_2H_4 in solution. It was washed first by ammonia solution in order to remove possibly existed unreduced $Ni(OH)_2$ [7], and then by de-ionized water to remove reaction residuals. The precipitate was further washed by acetone for drying. Finally, it was flushed with N_2 (containing about 1% O_2) at room temperature for 24 h in order to remove acetone and for passivation. The samples thus prepared were stable when exposed to air. The techniques of X-ray diffraction (XRD), Transmission Electron Micrograph (TEM) and BET measurement were used to determine the phase, particle size and surface area of the samples.

3. Results and discussion

3.1. Electrochemistry of the reduction

In aqueous solution, Ni^{2+}, H^+ and N_2H_4 are species that can be reduced as following:

$$Ni^{2+} + 2e^- = Ni \quad \varphi^{\emptyset} = -0.25\,V \tag{1}$$

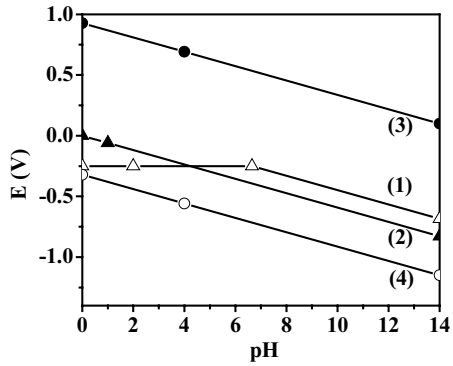

Figure 1 Electrode potentials of related half-reactions (cf. context).

$$2H_2O + 2e^- = H_2 + 2OH^- \quad \varphi^{\emptyset} = -0.83\,V \tag{2}$$

$$2N_2H_4 + 4H_2O + 4e^- = 4NH_3 + 4OH^- \quad \varphi^{\emptyset} = 0.1\,V \tag{3}$$

On the other hand, N_2H_4 is a strong reducing agent under basic medium:

$$N_2H_4 + 4OH^- = N_2 + 4H_2O + 4e^- \quad \varphi^{\emptyset} = -1.15\,V \tag{4}$$

By assuming the unit activity of Ni^{2+} and N_2H_4 in the solution, the pH dependence of the electrode potentials of these half reactions is plotted in Fig. 1. Fig. 1 shows that N_2H_4 is able to reduce Ni^{2+}, H^+ and itself under the pH from 0 to 14. However, its ability to reduce Ni^{2+} decreases with the decrease of pH. That is why the reduction of Ni^{2+} by N_2H_4 must be performed under the strong basic medium. By combining the half-reaction 4 with the half-reactions 1 to 3 , we obtained the following reactions:

$$2Ni^{2+} + N_2H_4 + 4OH^- = 2Ni\downarrow + N_2\uparrow + 4H_2O \tag{5}$$

$$N_2H_4 = N_2\uparrow + 2H_2\uparrow \tag{6}$$

$$3N_2H_4 = N_2\uparrow + 4NH_3\uparrow \tag{7}$$

The equilibrium constants of the reactions 5–7 are calculated to be 7×10^{60}, 4×10^{21} and 3×10^{84} according to the electrical potentials of these reactions. The great equilibrium constants indicate that the reactions are thermodynamically very favorable.

3.2. The main reaction versus the side reactions

The black precipitate formed during the reduction was confirmed to be metallic nickel by XRD. After a period of the reaction, the de-ionized water that used to absorb ammonia was tested by the Nessler agent. The Nessler agent turned to brown, confirming the production of ammonia. The gas after the removal of ammonia could be

TABLE I The volumes of the gases produced during the reaction

Reaction time (s)	V(N_2+H_2) (ml)	pH of NH_3 solution	V(NH_3) (ml)
0	0	7.58	0
168	52	8.16	0.046
6290 (end of reaction)	2004	11.08	423

Total gas volume = 2004 ml + 423 ml = 2427 ml.

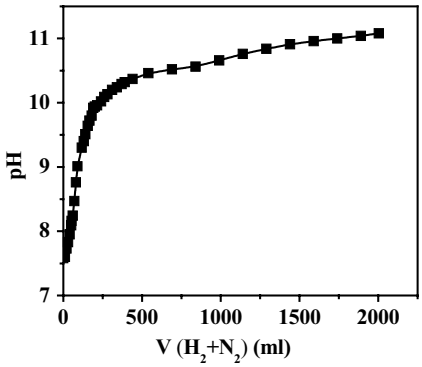

Figure 2 pH of the solution absorbed ammonia versus the volume of gases (N_2+H_2) evolved.

ignited, indicating the existence of H_2. These phenomena revealed that the reactions might proceed according to the Equations 5–7.

Since we recorded the pH of the solution that absorbed ammonia as well as the volume of the gas (without ammonia) versus time, we can plot the pH of the solution with the volume of the gas (N_2 + H_2), as shown in Fig. 2. Fig. 2 shows that the pH of the ammonia solution increased fast from 7.5 to 10 up to about 250 ml of the gas and then approached to 11 with the further increase of the gas volume up to about 2000 ml. According to the pH of the ammonia solution (200 ml), the volume of ammonia evolved can be calculated and given in Table I with the volume of N_2 + H_2 at the same time (0, 168 and 6290 s). It is seen that the volume of ammonia (0.046 ml) is much less than the volume of N_2 and H_2 (52 ml) at the reaction time of 168 s.

Since we used 0.0042 mol Ni^{2+} for a reaction with excess N_2H_4 (0.04 mol), the complete reduction of such amount of Ni^{2+} by N_2H_4 according to Equation 5 would consume 0.002103 mol N_2H_4 and produce 52 ml N_2. The excess gases produced are due to the side reactions 6 and 7. Since the total amount of ammonia produced during the reaction was measured to be 423 ml, the amount of hydrazine disproportionated to N_2 and NH_3 according to Equation 7 can be calculated to be 0.0128 mol, producing 105 ml N_2 and 423 ml NH_3, respectively. The remaining 0.02509 mol N_2H_4 would be consumed by the decomposition according to Equation 6 and produced 622 ml N_2 and 1243 ml H_2, respectively. Thus, the total volume of the gases calculated according to Equations 5–7 should be 2445 ml, agreeing well with the volume of the gases (2427 ml) measured experimentally. Table II summarizes the data about the consumption of hydrazine and the gases produced according to the reactions 5 – 7. Table II shows that only 5.3% hydrazine were consumed for the reduction of Ni^{2+}, while 62.7% hydrazine were decomposed to N_2 and H_2, and the other 32% hydrazine were converted to N_2 and NH_3 due to the disproportionation reaction.

Now that the reduction of 0.0042 mol Ni^{2+} consumed only 0.002103 mol N_2H_4 and produced 52 ml N_2, we stopped the reaction once it produced 52 ml gases. Upon filtration and washing of the black precipitate and analysis of the remaining Ni^{2+} in the residual solution, it was found that 99.7% Ni^{2+} had been reduced to nickel metal. At the same time, only 0.046 ml NH_3 formed, accounting for about 0.7% of N_2H_4 consumed by the reaction 7. In this case, the reaction 6 did not occur. These results showed that the overall reaction proceeded in two stages. The first stage is the reduction of Ni^{2+} by N_2H_4 according to 5 while the second stage is the decomposition of N_2H_4 6 and the disproportionation of N_2H_4 7 catalyzed by the product, metallic nickel. Therefore, we focused on the reaction kinetics for the reaction at the first stage below.

3.3. Reaction kinetics for the reduction of Ni^{2+}

The reaction between $NiCl_2$ and N_2H_4 in solution is a typical autocatalytic process. The rate equation can be written as,

$$r = \frac{dVt}{dt} = \frac{1}{2}\frac{dq}{dt} = k[Ni^{2+}]^{\alpha}[N_2H_4]^{\beta} + k'[Ni^{2+}]^{\alpha}[N_2H_4]^{\beta}q^{\gamma} \quad (8)$$

where r is the reaction rate, V_t the volume of gases produced up to time t, q the amount of product (Ni or Ni surface), k the rate constant for the non-catalytic reaction, k' the rate constant for the autocatalytic reaction, and α,

TABLE II Consumption of N_2H_4 and production of gases according to the reactions 5–7

Reaction	N_2H_4 consumption		V (N_2) (ml)	V(H_2) (ml)	V (NH_3) (ml)	V_{total} (ml) (calculated)
	n (mol)	%				
(5)	0.002103	5.3	52			
(6)	0.02509	62.7	622	1243		2445
(7)	0.01280	32.0	105		423	

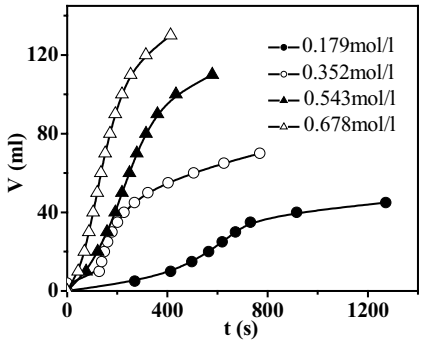

Figure 3 Volume of gases (N_2+H_2) evolved versus time with different initial concentrations of Ni^{2+} as indicated in the legend. Other conditions: $T = 288$ K, $[N_2H_4]_0 = 3.35$ mol/l, m(NaOH) = 2.5 g and the quantity of inducing agent ($NaBH_4$), $q_{ind} = 0.002$ g.

β, and γ are the reaction orders with respect to $[Ni^{2+}]$, $[N_2H_4]$ and q. Without the addition of an inducing agent, the reaction does not occur at 288 K, and therefore k is equal to 0. Then, the Equation 8 is simplified to be,

$$r = \frac{dVt}{dt} = \frac{1}{2}\frac{dq}{dt} = k'[Ni^{2+}]^{\alpha}[N_2H_4]^{\beta}q^{\gamma} \qquad (9)$$

Upon the addition of a small amount of the inducing agent, $NaBH_4$, the reaction occurred at 288 K. $NaBH_4$ is very active in reducing Ni^{2+} to produce Ni-B amorphous nano-particles [5] that catalyze the reaction between Ni^{2+} and N_2H_4 in the solution. Once the Ni-B nano-particles were produced (q), the reduction of Ni^{2+} by N_2H_4 at 288 K in the solution began, producing Ni nano-particles (also q) that catalyzed the reaction continuously. The reaction was accelerated when more and more Ni nano-particles (q) were produced. On the other hand, the concentration of Ni^{2+} decreased continuously with the proceeding of the reaction. The two factors determined that the volume of the gases evolved versus time displayed a sigmoid curve as shown in Fig. 3, characteristic of an autocatalytic reaction. Differentiation of such a curve gave the reaction rate versus time, which exhibited a maximum.

According to Equation 9, we write out an equation for the maximum rate,

$$r_{max} = k'[Ni^{2+}]^{\alpha}_{max}[N_2H_4]^{\beta}_{max}q^{\gamma}_{max} \qquad (10)$$

For the autocatalytic reaction, the following relations hold: $[Ni^{2+}]_{max} = A_1[Ni^{2+}]_0$, $[N_2H_4]_{max} = A_2[N_2H_4]_0$, $q_{max} = A_3q_0$, $q_0 = A_4q_{ind}$, where A_1, A_2, A_3 and A_4 are constants, $[Ni^{2+}]_0$, $[N_2H_4]_0$, and q_0 are the initial concentrations or quantities of the reactants and the catalyst, and q_{ind} the quantity of inducing agent. Substituting these relations for the items in Equation 10, we have,

$$r_{max} = k'A_1^{\alpha}[Ni^{2+}]_0^{\alpha}[N_2H_4]_0{}^{\beta}A_3{}^{\gamma}A_4{}^{\gamma}q_{ind}{}^{\gamma}$$

Keeping $[N_2H_4]_0$ and q_0 constant while varying $[Ni^{2+}]_0$, we have,

$$r'_{max} = k_1[Ni^{2+}]_0^{\alpha} \qquad (11)$$

Similarly, we obtain the following equations:

$$r''_{max} = k_2[N_2H_4]_0^{\beta} \qquad (12)$$

$$r'''_{max} = k_3q_{ind}^{\gamma} \qquad (13)$$

Or we have,

$$\ln r'_{max} = \ln k_1 + \alpha \ln[Ni^{2+}]_0 \qquad (11')$$

$$\ln r''_{max} = \ln k_2 + \beta \ln[N_2H_4]_0 \qquad (12')$$

$$\ln r'''_{max} = \ln k_3 + \gamma \ln q_{ind} \qquad (13')$$

While keeping $[N_2H_4]_0 = 3.35$ mol/l, m(NaOH) = 2.5 g and $q_{ind} = 0.002$ g at $T = 288$ K, we varied $[Ni^{2+}]_0$ (0.179, 0.352, 0.543 and 0.678 mol·dm^{-3}) and measured the volume of gases evolved versus time. The sigmoid curves obtained are displayed in Fig. 3, from which the maximum rates (r'_{max}) can be derived according to the slopes at the inflexion points of these curves. In Fig. 4 are shown the experimental results for the linear relations expressed by Equations 11′–13′. The reaction orders are then found to be about 1, 0 and 1 with respect to $[Ni^{2+}]$, $[N_2H_4]$ and q, i.e., $\alpha = 1$, $\beta = 0$ and $\gamma = 1$ in Equation 9.

Thus, the Equation 9 can be written as,

$$r = \frac{dVt}{dt} = \frac{1}{2}\frac{dq}{dt} = k'[Ni^{2+}]q \qquad (14)$$

Integration of Equation 14, we obtain,

$$\frac{1}{[Ni^{2+}]_0}\left\{\ln\frac{[Ni^{2+}]_0 - q_0}{q_0} + \ln\frac{q}{[Ni^{2+}]_0 - q}\right\} = k't$$

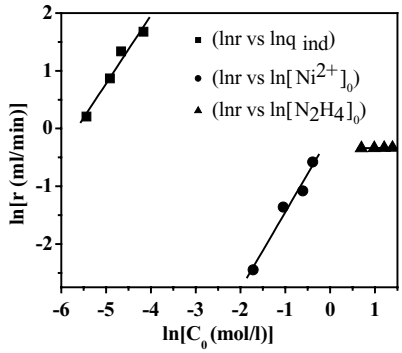

Figure 4 Logarithmic plots of reaction rates with respect to the initial concentrations of Ni^{2+}, N_2H_4 and inducing agent, q_{ind}.

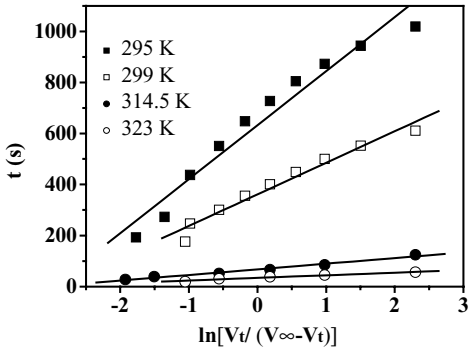

Figure 5 Plots of reaction time versus $\ln[V_t/(V_\infty - V_t)]$ according to Equation 15 for the reaction at different temperatures. Other conditions: $[Ni^{2+}]_0 = 0.35$ mol/l, m(NaOH) = 2.5 g and $[N_2H_4]_0 = 3.35$ mol/l.

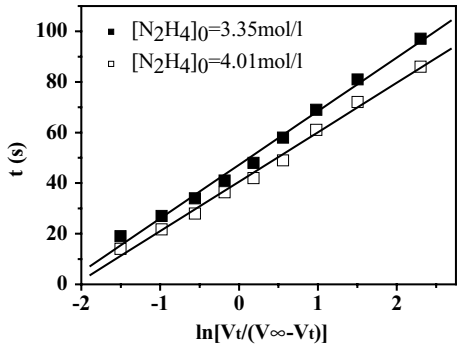

Figure 6 Plots of reaction time versus $\ln[V_t/(V_\infty - V_t)]$ according to Equation 15 for the reaction with different initial concentration of N_2H_4. Other conditions: $T = 299$ K, $[Ni^{2+}]_0 = 0.35$ mol/l and m(NaOH) = 2.5 g.

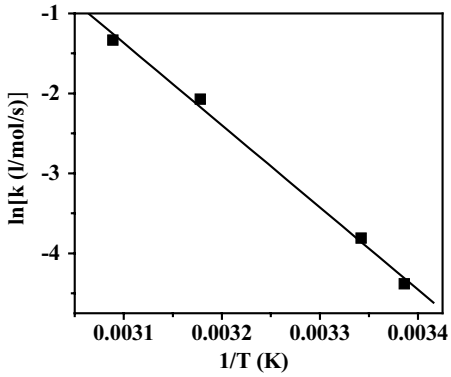

Figure 7 Arrhenius correlation for activation energy for the reduction of Ni^{2+} by hydrazine in solution.

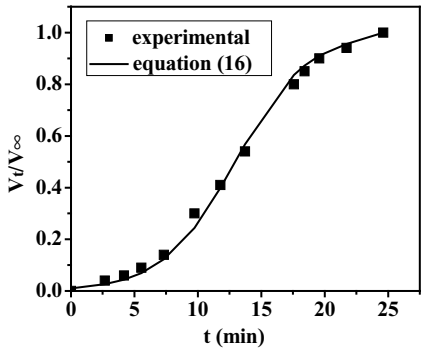

Figure 8 Kinetics of the reduction of Ni^{2+} by hydrazine in solution. Reaction conditions: $T = 288$ K, $[Ni^{2+}]_0 = 0.179$ mol/l, $[N_2H_4]_0 = 3.35$ mol/l, m(NaOH) = 2.5 g and the quantity of inducing agent ($NaBH_4$), q_{ind} = 0.002 g.

If we use V_t and V_∞ to represent the volumes of gases evolved at time t and at the end of reaction, respectively, we have,

$$\frac{q}{[Ni^{2+}]_0^{-q}} = \frac{v_t}{v_\infty - v_t}$$

And then we derive the following equation,

$$t = \frac{1}{k'[Ni^{2+}]_0} \ln \frac{[Ni^{2+}]_0 - q_0}{q_0} + \frac{1}{k'[Ni^{2+}]_0} \ln \frac{V_t}{V_\infty - V_t} \quad (15)$$

This equation demonstrates the linear relationship between t and $\ln \frac{V_t}{V_t - V_\infty}$. Accordingly, the rate constant k' can be obtained through the slope of the straight lines. In Figs 5 and 6 are shown the experimental results treated according to Equation 15 for the data obtained at different temperatures and different concentrations of N_2H_4. In both cases, the linear relationships are clearly seen, indicating that the Equation 15 is valid in describing the reduction of Ni^{2+} by N_2H_4 in the solution. According to the slopes ($= 1/k'[Ni^{2+}]_0$) of the lines in Fig. 5, reaction constants k' at different temperatures are obtained. Then, by using the Arrehnius correlation as shown in Fig. 7, the activation energy of the autocatalytic reaction was found to be 85 kJ mol^{-1}. The parallel lines in Fig. 6 indicate that the rate constant k' does not depend on the initial concentration of N_2H_4.

The constant $c = \{[Ni^{2+}]_0 - q_0\}/q_0$ in Equation 15 can be calculated according to the intercepts of the lines in Fig. 5 and 6. q_0 is the quantity of Ni–B catalyst produced by the addition of $NaBH_4$, and depends on the temperature and pH. The Equation 15 can be rearranged into,

$$\frac{V_t}{V_\infty} = \frac{1}{1 + \frac{[Ni^{2+}]_0 - q_0}{q_0} e^{-k'[Ni^{2+}]_0 t}} \quad (16)$$

Using the c value in Equation 16 for the certain reaction conditions ($T = 288$ K, $[Ni^{2+}]_0 = 0.179$ mol/l, m(NaOH) = 2.5 g and $[N_2H_4]_0 = 3.35$ mol/l), a plot of V_t/V_∞ versus time t can be obtained according to Equation 16 and is shown in Fig. 8. Fig. 8 shows that the Equation 16 fits the experimental data quite well. Fig. 8 also shows that the reaction completes in 24.6 min at the given reaction conditions.

When $V_t = 1/2V_\infty$, i.e., when the reaction proceeds half way, the Equation 15 becomes,

$$t_{1/2} = \frac{1}{k'[Ni^{2+}]_0} \ln \frac{[Ni^{2+}]_0 - q_0}{q_0}$$

Since $[Ni^{2+}]_0 \gg q_0$, we have,

$$t_{1/2} = \frac{1}{k'[Ni^{2+}]_0} \ln \frac{[Ni^{2+}]_0}{q_0} \quad (17)$$

When keeping $[Ni^{2+}]_0$ and q_0 constant, k' increases while $t_{1/2}$ decreases with the increase of temperature. Differentiating $t_{1/2}$ with respect to $[Ni^{2+}]_0$ and q_0 obtains the following inequalities,

$$\left[\frac{\partial t_{1/2}}{\partial [Ni^{2+}]_0}\right]_{q_0,k'} = \frac{1}{k'[Ni^{2+}]_0^2}\left(1 - \ln \frac{[Ni^{2+}]_0}{q_0}\right) < 0$$

$$\left[\frac{\partial t_{1/2}}{\partial q_0}\right]_{[Ni^{2+}]_0,k'} = -\frac{1}{k'[Ni^{2+}]_0 q_0} < 0$$

These inequalities indicate that the half life of the reaction, $t_{1/2}$, or the reaction rate decreases with the increase of $[Ni^{2+}]_0$ and q_0.

3.4. The ratio of N_2H_4/Ni^{2+} for the reduction

Ni *et al.* [14] used greatly excessive amount of N_2H_4 for the reduction of Ni^{2+}, in which only about 5% was used for the reduction of Ni^{2+} and the remaining N_2H_4 was decomposed into N_2, NH_3 and H_2, according to our results above. However, if we used the stoichiometric ratio of N_2H_4/Ni^{2+} (0.5) according to the reaction 5, we found that the reduction did not proceed. Further tests showed that the amount of N_2H_4 needed depended on the concentration of Ni^{2+}. With the increase of $[Ni^{2+}]_0$, the amount of N_2H_4 needed to reduce the same amount of Ni^{2+} decreased. This may be due to the fact that the reaction rate increased (or $t_{1/2}$ decreased) with the increase of $[Ni^{2+}]_0$, leading to the decrease of consumption of N_2H_4. Table III gives the experimental results. It is seen that the consumption of hydrazine decreased from 0.02 to 0.006 mol (or the ratio of $n(N_2H_4)/n(Ni^{2+})$ decreased from 4.8 to 1.5) when $[Ni^{2+}]_0$ increased from 0.68 to 1.10 mol/l, although the total amount of Ni^{2+} reduced was not changed. Therefore, by increasing the concentration of Ni^{2+}, the consumption of hydrazine can be greatly decreased. In any case, a ration of $n(N_2H_4)/n(Ni^{2+})$ as high as 10 used in [14] is not necessary according to our current work.

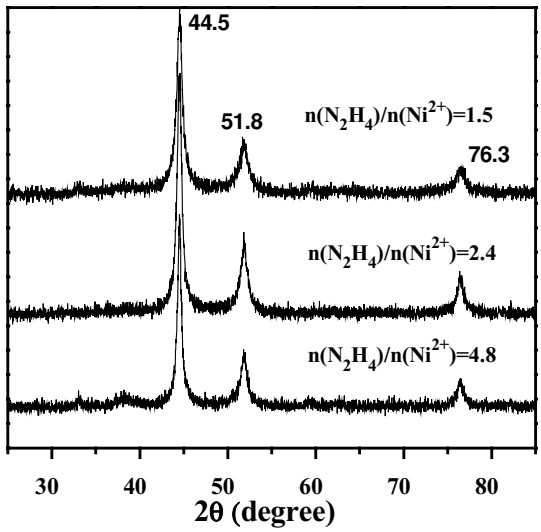

Figure 9 X-ray diffraction patterns of the samples precipitated by the reduction of Ni^{2+} with different $n(N_2H_4)/n(Ni^{2+})$ ratios as indicated.

3.5. Characterizations of precipitates

Fig 9 and 10 display the typical XRD pattern and TEM image of the precipitates formed by the reaction between Ni^{2+} and hydrazine in the solution. The XRD patterns exhibit the typical face-centered cubic structure of metallic nickel. No other species were clearly observed in the XRD pattern, indicating that pure nickel powders were obtained in our experiments. The surface areas of the samples prepared using different concentration of Ni^{2+} are given in Table III. The surface area was increased from 18 to 79 m^2/g with the increase of Ni^{2+} concentration from 0.68 to 1.10 mol/l, i.e., with the decrease of $n(N_2H_4)/n(Ni^{2+})$ ratio from 4.8 to 1.5. Accordingly, the XRD peaks were broadened with the increase of surface area (see Fig. 9). Calculations according to the Scherrer equation revealed that the particle sizes decreased from 13.8 to 8.4 nm for the samples with surface areas increased from 18 to 79 m^2/g, which were much smaller than those calculated according to the surface areas supposing that the particles are spherical (from 37 to 9 nm). The TEM graph shows that the sample with the

TABLE III Ratio of $n(N_2H_4)/n(Ni^{2+})$ versus the concentration of Ni^{2+}

					d (nm) according to	
$n(Ni^{2+})$ (mol)	$[Ni^{2+}]_0$ (mol·l^{-1})	$n(N_2H_4)$ (mol)	$n(N_2H_4)/n(Ni^{2+})$	BET (m^2/g)	Scherrer equation	BET
0.0042	0.35	0.04	10:1			
0.0042	0.68	0.02	4.8:1	18	13.8	37
0.0042	0.81	0.01	2.4:1	28	11.0	24
0.0042	1.10	0.006	1.5:1	79	8.4	9

Figure 10 Transmission electron micrograph of the sample precipitated by the reduction of Ni^{2+} with hydrazine in solution. Reaction conditions: T = 298 K, $[Ni^{2+}]_0 = 0.68$ mol/l, $[N_2H_4]_0 = 3.26$ mol/l and $m(NaOH) = 2.5$ g. BET area = 18 m^2g.

surface area of 18 m^2/g had an average particle size of about 30 nm, close to 37 nm calculated according to the surface area. These results seem to imply that the particles seen by TEM might contain smaller crystallites with sizes detected by Scherrer equation.

4. Conclusions

1. The reduction of Ni^{2+} by hydrazine in solution is composed of three reactions:

$$2Ni^{2+} + N_2H_4 + 4OH^- = 2Ni\downarrow + N_2\uparrow + 4H_2O \quad (5)$$

$$N_2H_4 = N_2\uparrow + 2H_2\uparrow \quad (6)$$

$$3N_2H_4 = N_2\uparrow + 4NH_3\uparrow \quad (7)$$

Electrochemically, the reactions must be carried out under strong basic medium. When excessive N_2H_4 is used, the reduction of Ni^{2+} by N_2H_4 as the reaction 5 occurs at the first stage and consumes only about 5% of N_2H_4 added when the ratio of $n(N_2H_4)/n(Ni^{2+})$ of 10 is used according to Ni *et al* [14]. The remaining N_2H_4 undergoes decomposition to N_2 and H_2, and disproportionation to N_2 and NH_3 catalyzed by the product nickel nano-particles. At the first stage, Ni^{2+} is completely reduced, while only negligible amount of N_2H_4 are disproportionated or decomposed.

2. When the stoichiometric ratio of $n(N_2H_4)/n(Ni^{2+})$ (0.5) is used according to the reaction 5, the reaction does not proceed. However, it was found that the amount of N_2H_4 needed to reduce the same amount of Ni^{2+} depends on the concentration of Ni^{2+}. For example, a ratio of $n(N_2H_4)/n(Ni^{2+})$ of 1.5 is sufficient to reduce completely the Ni^{2+} when the initial Ni^{2+} concentration is about 1 mol/l.

3. Kinetic studies reveal that the reduction of Ni^{2+} by N_2H_4 is an autocatalytic reaction. The nickel nano-particles produced during the reduction catalyzes the reduction reaction. Accordingly, if a small amount of inducing agent such as $NaBH_4$ is used, the reaction can proceed at 288 K. The reaction orders with respect to Ni^{2+}, N_2H_4 and Ni are found to be 1, 0 and 1, respectively. Thus, the increase of the initial concentration of Ni^{2+} and the amount of inducing agent used accelerate the reaction rate and decrease the consumption of N_2H_4. At the same time, the surface area of the produced nickel nano-particles are increased due to the more nuclei formed for the reduction of Ni^{2+}.

4. Pure nickel nano-particles with high surface areas (from 18 to 79 m^2/g) may be produced through the reduction of Ni^{2+} by N_2H_4 in the solution. The surface area of the nickel nano-particles was found to increase with the increase of concentration of Ni^{2+} used.

5. Outlook

Metallic nickel is an important catalyst widely used for hydrogenations. Preparing the porous Raney nickel or using a support is the usual ways to increase the number of surface nickel atoms. Sodium borohydride and hypophosphite are sometimes used to produce Ni-B and Ni-P nano-particles. When a support is used, the interaction between NiO and the support determines the reducibility of Ni^{2+} and the dispersion of nickel on the surface. Activated carbon (AC) has high surface areas with weak interactions with metal cations and metals. When nickel is supported on AC, the high reducibility is usually guaranteed, but the dispersion may not be high because of the weak interaction between nickel and the surface of carbon. On the other hand, NiO interacts strongly with the supports such as γ-Al_2O_3 and SiO_2, so that Ni^{2+} can be highly dispersed. Nevertheless, it is difficult to reduce such highly dispersed Ni^{2+}. The high temperatures that are used to reduce the Ni^{2+} on γ-Al_2O_3 and SiO_2 may lead to the sintering of the reduced nickel. The reduction of Ni^{2+} by N_2H_4 in basic solutions may provide a new way to prepare highly dispersed and reduced nickel catalysts supported on γ-Al_2O_3 and SiO_2. In fact, through the sol-gel method, Ni^{2+} can be highly dispersed in the sol, e.g., $(SiO_2)_m.nH_2O$, and are then reduced by N_2H_4. Upon washing, drying and heat treatment, a highly dispersed and reduced nickel catalyst supported on SiO_2 may be obtained.

Acknowlegments

Financial supports from Jiangsu Province (BG2002019) and from MSTC (2004DFB02900) are acknowleged.

References

1. S. C. DAVIS and K. J. KLABUNDE, *Chem. Rev.* **82** (1982) 157.
2. F. FIEVET, J. P. LAGIER and B. BLIN, *Solid State Ionics* **32** (1989) 198.
3. R. L. PECSOK, *J. Am. Chem. Soc.* **75** (1953) 2862.
4. R. C. WADE, D. G. HOLAH, A. N. HUGHES and B. C. HUI, *Catal. Rev.-Sci. Eng.* **14** (1976) 211.
5. J. SHEN, Z. LI, Q. YAN and Y. CHEN, *J. Phys. Chem.* **97** (1993) 8504.
6. S. SADA, *Kogyo Kagaku Zasshi* **71** (1968) 957.
7. J. SHEN, Z. HU, L. ZHANG, Z. LI and Y. CHEN, *Appl. Phys. Lett.* **59** (1991) 3545.
8. J. SHEN, Q. ZHANG, Z. LI and Y. CHEN, *J. Mat. Sci. Lett.* **15** (1996) 715.
9. Y. LI, L. LI, H. LIAO and H. WANG, *J. Mater. Chem.* **9** (1999) 2675.
10. Y. LI, C. LI, H. WANG, L. LI and Y. QIAN, *Mat. Sci. Commun.* **59** (1999) 88.
11. S. WU and D. CHEN, *J. Colloid Interf. Sci.* **259** (2003) 282.
12. A. DEGEN and J. MACEK, *Nano Struct. Mater.* **12** (1999) 225.
13. J. GAO, F. GUAN, Y. ZHAO, W. YANG and Y. MA, *Mater. Chem. Phys.* **71** (2001) 215.
14. X. NI, X. SU, Z. YANG and H. ZHENG, *J. Cryst. Grow.* **252** (2003) 612.
15. Z. GUI, R. FAN, W. MO, X. CHEN, L. YANG and Y. HU, *Mater. Res. Bull.* **38** (2003) 169.

Received 22 February
and accepted 27 July 2005